# Notes

## A Scaling Model for Osmotic Energy of Polymer Brushes

**H. Watanabe***

*Institute for Chemical Research, Kyoto University, Uji, Kyoto 611-0011, Japan*

**S. M. Kilbey, II**

*Department of Chemical Engineering, Clemson University, Clemson, South Carolina 29634*

**M. Tirrell**

*College of Engineering, University of California, Santa Barbara, California 93106*

*Received June 14, 2000*
*Revised Manuscript Received September 8, 2000*

### 1. Introduction

Polymer chains tethered densely on a substrate form a brush layer when swollen with a solvent, and the brush free energy $f_b$ has been measured in the surface force experiments of compressing two brushes tethered on opposing substrates.[1] These experiments revealed that the isolated brush is stretched, and the contact/compression of two brushes results in long-ranged repulsion.[1] The equilibrium height $L_{eq}$ of the isolated brush, evaluated as a half of the distance $D$ between the substrates at the onset of this repulsion, varies with the degree of polymerization $N$ and surface number density (grafting density) $\sigma$ of the brush chain. For a given $\sigma$, $L_{eq}$ is proportional to $N$.[1]

The stretched chain conformation (with $L_{eq} \propto N$) and the repulsion seen at $D < 2L_{eq}$ are related to the osmotic and elastic free energies of the brush (normalized to unit area of the substrate), $f_b^{os}$ and $f_b^{el}$. The $f_b^{os}$ increases while $f_b^{el}$ decreases with decreasing brush height $L$ (i.e., with increasing brush concentration $c$). Thus, $L_{eq}$ is determined as the $L$ that minimizes the total free energy $f_b$ ($= f_b^{os} + f_b^{el}$) of the isolated brush, and the repulsion represents the increase of $f_b$ on compression. In fact, the Patel−Tirrell−Hadziioannou (PTH) model[2] and the Milner−Witten−Cates (MWC) model[3] considered these features of the brushes and formulated $f_b$ in terms of the molecular parameters ($N$ and $\sigma$). These models successfully described the shape of the $f_b$−$D$ profile of the compressed brushes, except for a numerical prefactor of $f_b$ explained below.

Watanabe and Tirrell[4] examined $f_b$ for a series of poly(2-vinylpyridine)−polystyrene (PVP−PS) and poly(2-vinylpyridine)−polyisoprene (PVP−PI) diblock copolymers that were adsorbed on mica selectively at the PVP blocks. The nonadsorbed PS and/or PI blocks formed the brushes in toluene (a good solvent) and exhibited long-ranged repulsion.

* To whom correspondence should be addressed.

For comparison of these $f_b$ data with the predictions of the PTH and MWC models, Watanabe and Tirrell[4] first assumed that the osmotic pressure $\Pi$ is the same for the brush and semidilute solution having the same $c$. Under this assumption, they evaluated the osmotic $f_b^{os}$ (included in the models) from an empirical equation[5,6] for semidilute PS/toluene solutions,

$$\frac{\Pi M}{c k_B T N_A} = K_\Pi \left(\frac{c}{c^*}\right)^{1/(3\nu-1)} \quad \text{for } c^* < c < 0.15 \text{ g cm}^{-3} \tag{1}$$

with

$$c^* = \frac{M/N_A}{4\pi R_g^3/3}, \quad K_\Pi = 2.2 \text{ and } \nu = 0.595 \tag{2}$$

Here, $M$ is the chain molecular weight, $N_A$ is the Avogadro number, $k_B$ and $T$ are the Boltzmann constant and absolute temperature, and $c^*$ is the overlapping concentration defined with respect to the radius of gyration $R_g$ of an isolated chain. The proportionality constant $K_\Pi$ and the power-law exponent $\nu$ (characterizing $R_g \propto N^\nu$) of the PS/toluene solutions[5,6] have the values shown in eq 2.

For the above PS and PI brushes, Watanabe and Tirrell[4] found that the PTH and MWC models *underestimate* the $f_b$ data if the $f_b^{os}$ included in the models is faithfully evaluated from the $\Pi$ data of the semidilute solution (eq 1). They also found that the $f_b$ data are well-described by these models (in particular, by the MWC model at weak compression) *if* the $c^*$ included in eq 1 is replaced by $\beta c^*$ with $\beta = 0.58$, i.e., *if* the $\Pi$ data are multiplied by a factor $\beta' = \beta^{-1/(3\nu-1)} \cong 2.0$ and $f_b^{os}$ is calculated from this adjusted $\Pi$. (This adjustment also led to a change in the numerical prefactor of $f_b^{el}$.[4])

The above results suggest that the $c$ dependence of $f^{os}$ is the same for the brush and semidilute solution, but the magnitude of $f^{os}$ is larger for the brush by the factor $\beta' \cong 2.0$. In fact, this difference in the magnitude was unequivocally confirmed for the $f_b$ data at high compression where $f_b^{os} \gg f_b^{el}$ and the $f_b$ data were identical to the $f_b^{os}$ data. Direct comparison of these $f_b^{os}$ data with the $f_s^{os}$ data of the semidilute solutions (evaluated from the $\Pi$ data described by eq 1) revealed a relationship between $w^{-1}f_b^{os}$ and $w^{-1}f_s^{os}$ (the osmotic energies normalized by the total mass ($w$) of the chains),

$$\frac{w^{-1}f_b^{os}(c)}{w^{-1}f_s^{os}(c)} \cong 2 \tag{3}$$

This relationship, observed for the brushes irrespective of their $N$ and $\sigma$ values, was surmised to result from the difference of the chain conformations in the brush and semidilute solution:[4] Since $f^{os}$ reflects the segment−segment contacts determined by the chain conformation,

10.1021/ma0010377 CCC: $19.00 
Published on Web 11/10/2000

$f^{os}$ can be different for the tethered and untethered chains (in the brush and solution). However, no further discussion was made in ref 4 for the difference specified by eq 3.

This paper attempts to explain this difference quantitatively. For this purpose, we introduce a correlation length $\xi_b$ in the brush and derive, from a simple but self-consistent scaling argument, an expression of $\xi_b$ in terms of $N$, $\sigma$, and $c$. Then, we show that $f_b^{os}$ calculated from this $\xi_b$ is indeed larger than $f_s^{os}$ by a factor $\sim$2. Furthermore, we demonstrate that the use of this $f_b^{os}$ and the corresponding $f_b^{el}$ results in a change of the numerical prefactor of $f_b$ predicted from the PTH and MWC models but does not change the essential part of these models, i.e., the $L$ dependence of $f_b$ in a normalized form.

## 2. Model

**2.1. Difference of Π of Brush and Solution.** The empirical eq 1 describing the Π data of the semidilute solutions can be rewritten in terms of a characteristic length $\xi_s$ in the solution,

$$\Pi_s = K_\Pi \frac{k_B T}{4\pi\xi_s^3/3} \tag{4}$$

with

$$\xi_s = R_g\left(\frac{c}{c^*}\right)^{-\nu/(3\nu-1)} = \left(\frac{3m}{4\pi N_A}\right)^{\nu/(3\nu-1)} b^{-1/(3\nu-1)} c^{-\nu/(3\nu-1)} \tag{5}$$

Here, $m$ and $b$ ($=R_g/N^\nu$) are the molecular weight and size of the monomer. Within the semidilute blob scheme,[7] eq 4 suggests that the chain is composed of blobs of the radius $\xi_s$ and each blob (having the volume $4\pi\xi_s^3/3$) sustains the osmotic energy $K_\Pi k_B T$. We hereafter refer to $\xi_s$ as the correlation length. (Our $\xi_s$ is a half of the conventionally used correlation length, the blob diameter.)

The Π in the semidilute regime (eq 4) reflects the segment−segment contacts of overlapping chains. Thus, $\xi$ should be different for the chains having different conformations in the brush and solution. To demonstrate this difference, we here utilize the PTH model and indicate that an inconsistency prevails if we *assume* the identity of $\xi$'s in the brush and solution.

The PTH model[2] adopts the Alexander−de Gennes hypothesis[8,9] that the chain concentration is uniform throughout the brush and the free ends of the chains are located at the tip of the brush. In the more elaborated MWC model[3] that self-consistently calculates the chain end distribution, the brush has a parabolic concentration profile. However, this difference between the PTH and MWC models does not affect the conclusion about the inconsistency deduced below.

Under the *assumption* that $\xi$ is the same for the brush and solution, $\Pi_b$ and $\xi$ of the brush are described by eqs 4 and 5 with $c$ in eq 5 being replaced by $w_0/L$. Here, $w_0$ is the mass of the tethered chains per unit area of the substrate; $w_0 = mN\sigma/N_A$. Integrating this $\Pi_b$ with respect to $L$, we obtain the osmotic $f_b^{os}$. Similarly, the elastic $f_b^{el}$ is evaluated as an elastic energy of $\sigma$ Gaussian chains, each being composed of blobs of the diameter $2\xi_s$. Minimization of $f_b$ ($= f_b^{os} + f_b^{el}$) with respect to $L$ gives the equilibrium brush height of the PTH model under the above assumption,[4,10]

$$L_{eq} = Q_s b^{1/\nu} \sigma^{(1-\nu)/2\nu} N \tag{6}$$

with

$$Q_s = \left[\frac{2^{(6\nu-1)/2\nu}(3\nu-1)K_\Pi}{3^{(2\nu-1)/2\nu}(4\nu-1)}\right]^{(3\nu-1)/4\nu}\left(\frac{4\pi}{3}\right)^{(1-\nu)/2\nu}$$

Here, we have approximated the root-mean-square end-to-end distance $R_e$ as $R_e \cong 6^{1/2}R_g = 6^{1/2}bN^\nu$.

From eq 6, the equilibrium concentration in the isolated brush is calculated to be $c_{eq} = w_0/L_{eq} = \{m\sigma^{(3\nu-1)/2\nu}\}/\{N_A Q_s b^{1/\nu}\}$. This $c_{eq}$ is *smaller* than $c^*$ (eq 2) if $\sigma < G\sigma^* \cong 9.7\sigma^*$ (for $\nu = 0.595$ and $K_\Pi = 2.2$). Here, $\sigma^* = 1/(\pi R_e^2)$ is the critical grafting density above which the tethered chains are crowded on the substrate to form the brush, and $G = (9/2)(3/4\pi)^{(1-\nu)/(3\nu-1)}Q_s^{2\nu/(3\nu-1)}$. This result indicates an *inconsistency* that the chains having $\sigma/\sigma^* = 1-9.7$ are crowded on the substrate but has $\Pi(c) < \Pi(c^*)$ where $\Pi(c^*)$ is the *minimum* Π value for the crowded (semidilute) chains.

The $L_{eq}$ of the MWC model[3] is larger than the $L_{eq}$ of the PTH model (eq 6). Thus, the average concentration in the isolated brush predicted from the MWC model is smaller than $c_{eq}$ of the PTH model, meaning that the above inconsistency becomes more prominent for the MWC model.

This inconsistency results from the wrong, starting assumption that $\xi$ is the same in the brush and semidilute solution. The untethered chains in the solution have a freedom of translation in all directions so that their crowdness (reflected in Π) is scaled by the $c/c^*$ ratio. In contrast, the tethered chains in the brush have no freedom of translation in the direction normal to the substrate. Thus, the chains are more easily crowded on the substrate than in the solution, thereby having smaller $\xi(c)$ and larger $\Pi(c)$ in the brush.

**2.2. Correlation Length in Brush.** Considering the above inconsistency, we here introduce a correlation length (blob radius) $\xi_b$ in the semidilute brush. In analogy to eq 4 for the semidilute solution, we can express $\Pi_b$ of the brush in terms of this $\xi_b$,

$$\Pi_b = K_\Pi \frac{k_B T}{4\pi\xi_b^3/3} \tag{7}$$

Here, the prefactor $K_\Pi$ (= 2.2) is identical to that for the solution.

Now, we introduce a scaling form for $\xi_b$ of the brush having the concentration $c$,

$$\xi_b = \xi_{b,r}\left(\frac{c}{c_r}\right)^{-\alpha} \tag{8}$$

Here, $\xi_{b,r}$ is a characteristic length of the brush in a certain reference state at the concentration $c_r$, and α is the scaling exponent (with its value being determined from later argument). As the simplest choice, the unstretched layer of the tethered chains having $\sigma^*$ can be utilized as this reference state; cf. Figure 1a. However, the concentration in this layer is heterogeneous in the lateral direction (because of the dilute zone between the chains having the so-called mashroom conformation;[1] see the shaded zone in Figure 1a). This heterogeneity results in an uncertainty in the evaluation

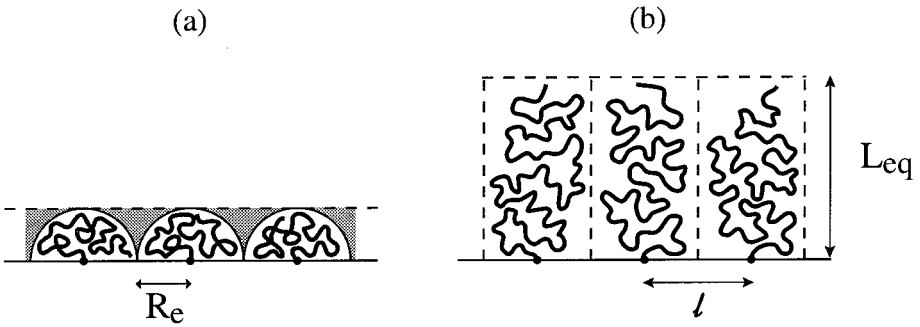


**Figure 1.** Schematic illustration of (a) tethered chains having the critical grafting density $\sigma^* = 1/\pi R_e^2$ and (b) chains having $\sigma > \sigma^*$ and forming the stretched brush. A characteristic length in the uncompressed brush (part b) is given by $l = \sigma^{-1/2}$.

of $c_r$. Thus, for definiteness, we choose a different reference state.

Concerning this choice, we note an interesting feature of the scaling expression, eq 8. For a given choice of a reference state having $\xi_{b,r}$ at $c_r$, the correlation length at a concentration $c'$ is written as $\xi_b' = \xi_{b,r}\,(c'/c_r)^{-\alpha}$. Utilizing these $\xi_b'$ and $c'$ in eq 8, we can express the $\xi_b$ at any $c$ in the same functional form, $\xi_b = \xi_b'(c/c')^{-\alpha}$. Namely, the scaling result is insensitive to our choice of the reference state. This type of insensitivity is common for all scaling arguments.

Here, it is informative to remember how the local concentration $c_l$ in the random coil of the chain changes with the solution concentration $c$: $c_l$ begins to increase with increasing $c$ above $c^*$. Thus, the solution at $c^*$ is naturally chosen as the reference state, and the chain dimension $R_g$ in this reference solution is utilized as the reference length in the scaling expression, eq 5.

The increase of $c_l$ in the opposing brushes (the situation in surface force experiments) is achieved by compression; however, the brush chains are already crowded on the substrate in the uncompressed state. Thus, in analogy to the above choice for the solution, the uncompressed (isolated) brush having no lateral heterogeneity of $c_l$ is naturally chosen as the reference for the compressed brush. The reference insensitivity of the scaling result allows us to make this choice.

With the above choice for the brush, eq 8 can be rewritten as

$$\xi_b = Bl\left(\frac{c}{c_{eq}}\right)^{-\alpha} = Bl\left(\frac{L}{L_{eq}}\right)^{\alpha} \quad \text{with } l = \sigma^{-1/2} \tag{9}$$

Here, $c_{eq}$ is the equilibrium concentration in the uncompressed brush, and $l$ is a characteristic distance between the grafting points on the substrate; cf. Figure 1b. This $l$ is proportional to but not necessarily identical to the reference length ($= \xi_b$ at $c_{eq}$). The proportionality constant $B$ in eq 9 accounts for this numerical difference between $l$ and the reference length ($Bl$). This length is analogous to $R_g$ of the untethered chain in the solution at $c^*$. The $B$ value is later determined on the basis of this analogy.

The semidilute blob scheme[7] suggests that $\xi_b$ of the compressed brush is determined locally. Thus, $\xi_b$ at $c > c_{eq}$ should be dependent on $c$ but not on the parameters related to the global chain conformation, $N$ and $l$. The exponent $\alpha$ in eq 9 is determined from these $l$- and $N$-independence requirements for $\xi_b$. Since $c_{eq}$ in eq 9 is given by $mN\sigma/N_A L_{eq}$ and $L_{eq}$ is dependent on $\sigma$, $N$, and $\alpha$, the determination of the $\alpha$ value requires a full analysis of $f_b^{os}$ and $f_b^{el}$ described below.

**2.3. Analysis of Brush Energy.** We follow the treatment in the PTH model[2] and make the analysis for the flat, Alexander−de Gennes-type brush[8,9] having the uniform concentration $c = c_{eq}L_{eq}/L$. In the followings, we determine the $\alpha$ and $B$ values (cf. eq 9) and then obtain an expression of $f_b^{os}$.

As noted from eq 9, determination of $\alpha$ requires us to specify $L_{eq}$ for which $f_b$ ($= f_b^{os} + f_b^{el}$) of the isolated brush is minimized. For calculation of $f_b^{os}$, we utilize eq 9 to rewrite eq 7 as $\Pi_b(L) = \{3k_BTK_\Pi L_{eq}^{3\alpha}\}/\{4\pi B^3 l^3 L^{3\alpha}\}$. Integration of this $\Pi_b$ gives[11]

$$f_b^{os}(L) = -\int_\infty^L \Pi_b\, dL = \frac{3k_BTL_{eq}^{3\alpha}K_\Pi}{4\pi(3\alpha - 1)B^3l^3L^{3\alpha-1}} \tag{10}$$

For calculation of $f_b^{el}$, we regard the brush chain as a Gaussian chain composed of blobs of the diameter $2\xi_b$. Each blob contains $(2\xi_b/a)^{1/\nu}$ monomers with $a$ ($\cong 6^{1/2}b$) being the effective step length of the monomer, and the blob number in each chain is $n = N/(2\xi_b/a)^{1/\nu}$. Thus, $f_b^{el}$ is given by $f_b^{el} = (3/2)\sigma k_BTL^2/n(2\xi_b)^2$.[2,4] With the aid of eq 9, this $f_b^{el}$ is rewritten as

$$f_b^{el}(L) = \frac{3k_BTB^{(1-2\nu)/\nu}L_{eq}^{(2\alpha\nu-\alpha)/\nu}}{2^{(3\nu-1)/\nu}a^{1/\nu}l^{(4\nu-1)/\nu}NL^{(2\alpha\nu-2\nu-\alpha)/\nu}} \tag{11}$$

Requiring $f_b$ (a sum of these $f_b^{os}$ and $f_b^{el}$) to be minimized at $L = L_{eq}$, we find

$$L_{eq} = Q_b a^{1/\nu} l^{(\nu-1)/\nu} N \quad \text{with } Q_b = \frac{2^{(\nu-1)/\nu}K_\Pi \nu}{\pi(2\nu + \alpha - 2\alpha\nu)B^{(1+\nu)/\nu}} \tag{12}$$

This $L_{eq}$ is utilized in eq 9 to give an expression of $\xi_b$,

$$\xi_b = BQ_b^{-\alpha}\left(\frac{m}{N_A}\right)^{\alpha} a^{-\alpha/\nu} l^{(\alpha+\nu-3\alpha\nu)/\nu} N^0 c^{-\alpha} \tag{13}$$

Here, $Q_b$ is the numerical factor given by eq 12. This $\xi_b$ is required to be independent of $N$ and $l$. The $N$-independence requirement is automatically satisfied in eq 13, and the $l$-independence requirement determines the $\alpha$ value,

$$\alpha = \frac{\nu}{3\nu - 1} \tag{14}$$

Interestingly, this $\alpha$ value, derived from our scaling analysis, is identical to the exponent value for $\xi_s$ in the semidilute solution (eq 5).

Equations 12 and 14 give an explicit relationship between $c_{eq} = mN\sigma/N_A L_{eq}$ and $B$,

$$c_{eq} = \frac{2^{(1-\nu)/\nu}(4\nu - 1)\pi m B^{(1+\nu)\nu}}{(3\nu - 1)N_A K_\Pi a^{1/\nu} f^{(3\nu-1)/\nu}} \quad (15)$$

We utilize this $c_{eq}$ to determine the $B$ value. For this purpose, we remember the meaning of the reference state. For the untethered chains in this state, the solution concentration coincides with the concentration in the isolated coil, $c^* = (Nm/N_A)/(4\pi R_g{}^3/3)$. For the tethered chains, the blob radius $Bl$ in the reference (uncompressed) brush plays the same role as the $R_g$ of the untethered chains; cf. eqs 5 and 9. Thus, $c_{eq}$ of this reference brush should coincide with the concentration in the blob, $c_{blob} = \{(2Bl/a)^{1/\nu} m/N_A\}/\{4\pi(Bl)^3/3\}$. This argument gives

$$B = \left[\frac{3(3\nu - 1)K_\Pi}{2\pi^2(4\nu - 1)}\right]^{1/4} \quad (= 0.66 \text{ for } K_\Pi = 2.2 \text{ and } \nu = 0.595) \quad (16)$$

From eqs 10, 14, and 16, we finally find an explicit expression of $f_b^{os}$ of the compressed brush in terms of $c$ and $w_0$ ($= mN\sigma/N_A = mN/N_A l^2$),

$$f_b^{os}(c) = (3\nu - 1)k_B T Q_b{}'\left(\frac{m}{N_A}\right)^{-3\nu/(3\nu-1)} a^{3/(3\nu-1)} w_0 c^{1/(3\nu-1)} \quad (17)$$

with

$$Q_b{}' = K_\Pi\left(\frac{\pi}{6}\right)^{1/(3\nu-1)} = 0.965 \quad \text{for } K_\Pi = 2.2 \text{ and } \nu = 0.595 \quad (18)$$

This $f_b^{os}$, calculated for the Alexander−de Gennes-type brush having the correlation length $\xi_b$, is to be consistently compared with $f_s^{os}$ calculated for the same type of brush having the solution correlation length $\xi_s$. Integrating $\Pi_s$ (eq 4) with respect to $L$, we can readily calculate this $f_s^{os}$ as

$$f_s^{os}(c) = (3\nu - 1)k_B T Q_s{}'\left(\frac{m}{N_A}\right)^{-3\nu/(3\nu-1)} a^{3/(3\nu-1)} w_0 c^{1/(3\nu-1)} \quad (19)$$

with

$$Q_s{}' = K_\Pi\left(\frac{2^{1/2}\pi}{3^{5/2}}\right)^{1/(3\nu-1)} = 0.445 \quad \text{for } K_\Pi = 2.2 \text{ and } \nu = 0.595 \quad (20)$$

Equations 17−20 indicate that $f_b^{os}$ and $f_s^{os}$ have the same $c$ dependence but the magnitude is larger for the former by a factor

$$\frac{w_0{}^{-1} f_b^{os}(c)}{w_0{}^{-1} f_s^{os}(c)} = \frac{Q_b{}'}{Q_s{}'} = 2.17 \quad (\text{for } \nu = 0.595) \quad (21)$$

This result is consistent with the experimental observation (eq 3).

The difference specified by eq 21 reflects a difference between $\xi_b$ and $\xi_s$. Comparing $\xi_b$ (eq 13 with eqs 14 and 16) with $\xi_s$ (eq 5), we find $\xi_b/\xi_s = (2/3)^{1/(6\nu-2)}$ (= 0.772 for $\nu = 0.595$). Namely, $\xi_b$ and $\xi_s$ exhibit the same $c$ dependence, but the magnitude is smaller for $\xi_b$ (to give $f_b^{os} > f_s^{os}$) because of the enhanced segment−segment contact due to the tethered brush ends. This enhancement is reflected in the factor $Bl$ in eq 9.

**2.4. Force−Distance Profile.** Surface force experiments utilize two curved surfaces to measure the force $F(D)$ between the opposing brushes thereon as a function of the surface separation $D$.[12,13] Usually, the surface curvature $R$ is orders of magnitude larger than the brush height. Then, the Derjaguin approximation[14] is valid, and the $F(D)$ data for the two identical, mutually compressed brushes are related to the free energy $f_b(L)$ of each brush as $F(D)/R = 4\pi\{f_b(L) - f_b(L_{eq})\}$.[1,2]

The PTH and MWC models underestimate the $F/R$ data if the $f_b^{os}$ and $f_b^{el}$ in the models are calculated from $\xi_s$ (eq 5).[4] Here, we utilize the $f_b^{os}$ (eq 17) and $f_b^{el}$ (eq 11 with eqs 12, 14, and 16), both calculated from $\xi_b$, and reformulate the PTH model: Following the treatment in the PTH model, we assume that the compressed brushes do not penetrate each other. (We do not consider extremely high compression that induces this mutual penetration.) Then, $D$ is simply given by $2L$, and the $D$ dependence of $F/R$ is readily found.

Following the previous study,[4] we introduce the reduced force $\mathcal{F}$ and reduced distance $\mathcal{D}$,

$$\mathcal{F} = \frac{F/R}{k_B T \sigma^{(2\nu+1)/2\nu} b^{1/\nu} N} \quad \text{and} \quad \mathcal{D} = \frac{D}{2\sigma^{(1-\nu)/2\nu} b^{1/\nu} N} \quad (22)$$

From eqs 11, 12, 14, 16, and 17, we find a relationship between $\mathcal{F}$ and $\mathcal{D}$ of the PTH model,

$$\mathcal{F}(\mathcal{D};\xi_b) = X_b\left[\left\{\left(\frac{D}{D_b^{eq}}\right)^{-1/(3\nu-1)} - 1\right\} + \frac{1}{4\nu - 1}\left\{\left(\frac{D}{D_b^{eq}}\right)^{(4\nu-1)/(3\nu-1)} - 1\right\}\right] \quad (23)$$

with

$$X_b = 2^{(8\nu-1)/4\nu} 3^{1/4\nu} \pi^{(2\nu+1)/2\nu}(4\nu - 1)\left[\frac{(3\nu - 1)K_\Pi}{4\nu - 1}\right]^{(4\nu-1)/4\nu} \quad (24)$$

and

$$D_b^{eq} = 2^{(5\nu-1)/4\nu} 3^{(1-\nu)/4\nu} \pi^{(1-\nu)/2\nu}\left[\frac{(3\nu - 1)K_\Pi}{4\nu - 1}\right]^{(3\nu-1)/4\nu} \quad (25)$$

Here, $D_b^{eq}$ is the reduced distance at the onset of repulsion. Since $X_b$ and $D_b^{eq}$ are independent of $N$ and $\sigma$, $\mathcal{F}$ is universally dependent on $\mathcal{D}$ irrespective of the $N$ and $\sigma$ values (cf. eq 23).

For the PTH model formulated on the basis of $\xi_s$, $\mathcal{F}(\mathcal{D};\xi_s)$ is written in the form of eq 23 with $X_b$ and $D_b^{eq}$ being replaced by

$$X_s = 2^{(16\nu^2+2\nu+1)/8\nu^2} 3^{-(2\nu+1)/8\nu^2} \pi^{(2\nu+1)/2\nu}(4\nu - 1) \times \left[\frac{(3\nu - 1)K_\Pi}{4\nu - 1}\right]^{(4\nu-1)/4\nu} \quad (26)$$

and

$$D_s^{eq} = 2^{(10\nu^2-\nu+1)/8\nu^2} 3^{-(2\nu^2-\nu+1)/8\nu^2} \pi^{(1-\nu)/2\nu} \times \left[\frac{(3\nu-1)K_\Pi}{4\nu-1}\right]^{(3\nu-1)/4\nu} \quad (27)$$

This $F(D;\xi_s)$ is also universally dependent on $D$.

## 3. Discussion

**3.1. Feature of $f_b^{os}$ and $f_s^{os}$.** The $f_b^{os}$ and $f_s^{os}$ (eqs 17 and 19) were commonly calculated from a particular model (PTH model). However, the conclusions deduced from this calculation, i.e., the coincidence of the $c$ dependencies of $f_b^{os}$ and $f_s^{os}$ and the difference in their magnitude (eq 21), appear to be valid in general.

Concerning this point, we should emphasize that the scaling exponent $\alpha$ for $\xi_b$ (eq 9) was not assumed, but self-consistently calculated from the argument that $\xi_b$ in the compressed brush is locally determined and thus independent of $l$ and $N$. The resulting $\alpha$ (eq 14) coincides with the scaling exponent for $\xi_s$, leading to the coincidence of the $c$ dependencies of $f_b^{os}$ and $f_s^{os}$.

We should also emphasize the difference between the intrinsic length scales in the brush ($Bl$; cf. eq 9) and solution ($R_g$; cf. eq 5). Because of this difference, the chains begin to be crowded at lower $c$ in the brush than in the solution. Consequently, $f^{os}$ is larger in the brush than in the semidilute solution having the same $c$, as noted from the calculation (eq 21) and experiments (eq 3).

**3.2. Comparison with Experiments.** Figure 2 shows the surface force data of PVP−PS and PVP−PI brushes (adsorbed on mica at the PVP blocks) in toluene.[4] The data are shown as plots of $F$ against $D$ (cf. eq 22). The plots for the brushes having various $N$ and $\sigma$ values (shown with various symbols) are collapsed into the universal curve. This collapse (universal $D$ dependence of $F$) is expected from the PTH and MWC models formulated on the basis of either $\xi_s$ or $\xi_b$.

In Figure 2, the thin dotted curve indicates the $F(D;\xi_s)$ of the PTH model *calculated from* $\xi_s$ (eq 23 with $X_b$ and $D_b^{eq}$ being replaced by $X_s$ (eq 26) and $D_s^{eq}$ (eq 27)). This model underestimates the $F$ data. At high compression where the $F$ data are dominantly contributed from the osmotic energy, this underestimation is quantified by eq 3. The same underestimation was noted for the MWC model (because the PTH and MWC models predict the same $F$ at high compression).[4]

The thick solid curve indicates the $F(D;\xi_b)$ of the PTH model (eqs 23−25). The $F(D;\xi_b)$ curve of the MWC model[15] is shown with the thick dashed curve. The data are close to these model curves calculated from $\xi_b$, in particular to the MWC curve at weak compression. This result suggests that the surface force data are quantitatively described by these models (with no adjustable parameter) if the properly evaluated correlation length ($\xi_b$) is utilized in the models.

## 4. Concluding Remarks

In this study, we have demonstrated that the correlation length $\xi$ and the corresponding osmotic free energy $f^{os}$ are different for the polymer brush and semidilute solution. This difference reflects enhanced segment−segment contact due to the tethered brush ends. Scaling calculation suggested that the $f_b^{os}$ and $f_s^{os}$ of the brush and solution have the same $c$ dependence but different magnitudes; $f_b^{os}(c)/f_s^{os}(c) \cong 2.2$. These results are consistent with experiments.

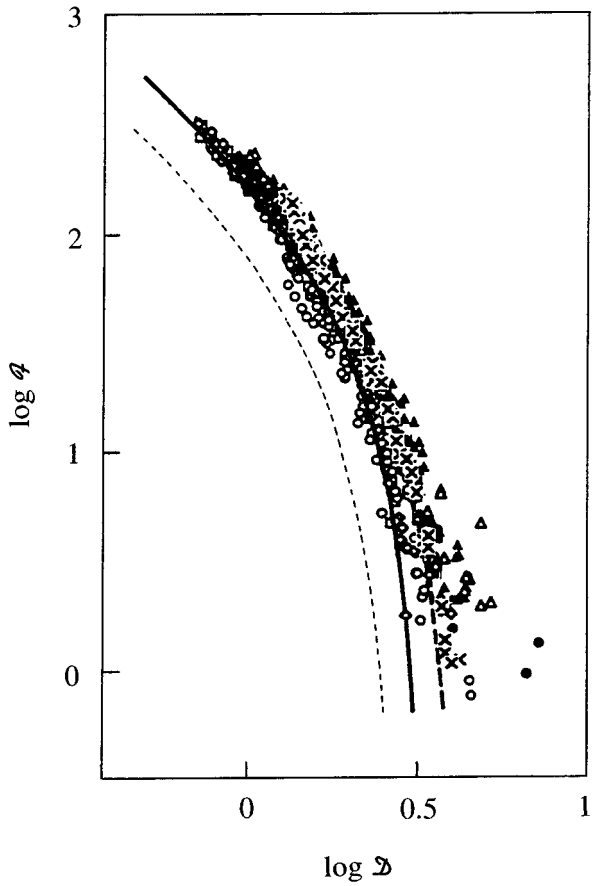


**Figure 2.** Force−distance profile of various PVP−PS and PVP−PI brushes in toluene obtained in the previous work.[4] Different symbols stand for the brushes having different molecular weights and/or grafting densities. The profile is shown as double-logarithmic plots of the reduced force $F$ against the reduced distance $D$. (The previous work[4] used symbols **f** and $\partial$ instead of $F$ and $D$.) The thin dotted curve indicates the $F$ predicted from the PTH model formulated on the basis of $\xi_s$. The thick, solid and dashed curves represent the prediction of the PTH and MWC models reformulated on the basis of $\xi_b$.

We have also utilized the brush correlation length $\xi_b$ to reformulate the PTH and MWC models. The predicted surface forces are in good agreement with the data. This result suggests the validity of the models utilizing the proper correlation length.

**Acknowledgment.** H.W. acknowledges, with thanks, financial support to this work from Japan Chemical Innovation Institute (through the Doi Project for development of Platform for designing high functional materials). M.T. acknowledges support of the National Science Foundation (Grant NSF-CTS-9616797).

## References and Notes

(1) For comprehensive summary of the structures/properties of tethered chains, see: Halperin, A.; Tirrell, M.; Lodge, T. *Adv. Polym. Sci.* **1992**, *100*, 31.
(2) Patel, S.; Tirrell, M.; Hadziioannou, G. *Colloids Surf.* **1988**, *31*, 157.
(3) Milner, S. T.; Witten, T. A.; Cates, M. E. *Macromolecules* **1988**, *21*, 2610.
(4) Watanabe, H.; Tirrell, M. *Macromolecules* **1993**, *26*, 6455.
(5) Noda, I.; Kato, N.; Kitano, T.; Nagasawa, M. *Macromolecules* **1981**, *14*, 668.

(6) Noda, I.; Higo, Y.; Ueno, N.; Fujimoto, T. *Macromolecules* **1984**, *17*, 1055.
(7) de Gennes, P.-G. *Scaling Concepts in Polymer Physics*, Cornel University Press: Ithaca, NY, 1977; Chapter III.
(8) Alexander, S. *J. Phys.* (*Paris*) **1977**, *38*, 977, 983.
(9) de Gennes, P.-G. *J. Phys.* (*Paris*) **1976**, *37*, 1443; *Macromolecules* **1980**, *13*, 1069.
(10) In the previous analysis,[4] the blob diameter (conventionally used correlation length) was considered to coincide with $R_e$ at $c = c^*$. The resulting $L_{eq}$ (calculated from $\xi_s$) was also written in the form of eq 6 and had a prefactor $Q_s = [4(3\nu - 1)K_\Pi/(4\nu - 1)]^{(3\nu-1)/4\nu}$. This $Q_s$ is larger than that given in eq 6 only by a factor $[(3/2)^{(2\nu-1)/2\nu}]^{(3\nu-1)/4\nu} = 1.02$ (for $\nu = 0.595$). Thus, the $L_{eq}$'s obtained in this and previous studies are very close to each other.
(11) The integral conducted in eq 10 calculates the work per unit area that has to be done against the osmotic pressure to compress the brush to the height, $L$.[4]
(12) Israelachvili, J. N.; Adams, G. E. *J. Chem. Soc., Faraday Trans. 1* **1978**, *74*, 975.
(13) Strictly speaking, $D$ is the separation between the substrates corrected for a small thickness of the tethering portion, e.g., the thin adsorbed PVP layer for the case of PVP−PS brushes.[4]
(14) Derjaguin, B. V. *Kolloid Z.* **1934**, *69*, 155.
(15) For the PTH model, we find a relationship between $F$'s calculated from $\xi_b$ and $\xi_s$, $F(D;\xi_b) = x_r F(D/d_r;\xi_s)$ with $x_r = X_b/X_s$ and $d_r = D_b^{eq}/D_s^{eq}$ (cf. eqs 23−27). The same relationship holds also for the MWC model. Applying this relationship to $F_{MWC}(D;\xi_s)$ of the MWC model calculated from $\xi_s$,[4] we obtained $F_{MWC}(D;\xi_b)$ of this model reformulated on the basis of $\xi_b$ (thick dashed curve in Figure 2).

MA0010377